A Coordinated Control Strategy for DC-link Voltage and Crowbar to Enhance Low Voltage Ride-Through of DFIG-based Wind Energy Conversion Systems

Tan Luong Van, *Member, IEEE*, Trung Hieu Truong, Hoan Tran, Ngoc Khoa Dang

Abstract -***This paper proposes a coordinated control strategy for DC-link voltage and crowbar for low voltage ride-through (LVRT) of partially-rated converter-based wind turbine with energy storage system (ESS) and crowbar connected to DC-link bus. With the proposed method, the DC-link voltage is controlled by the ESS, while the grid-side converter (GSC) is emploited to control the reactive power according to the grid code requirements. Also, the crowbar has been used to dissipate the surplus power between the rotor and ESS. The validity of the proposed system is verified by simulation results for a 2-MW doubly-fed induction generator (DFIG) wind turbine system*.**

Keywords: ***Crowbar, doubly-fed induction generator, energy storage system, ride-through, wind turbine.***

I. INTRODUCTION

In recent decades, variable-speed wind turbines with a DFIG are widely used in the field due to its advantage of operation with the excitation converter rated at only 25%-30% of generator power rating. The performance of the DFIG –based wind turbine system in the normal condition is currently well understood [l].

Recently, some nations have issued the dedicated grid codes to connect the wind turbine system with the electric grid [2]-[5]. Also, the micro-grid and the smart-grid systems have been studied for management of the power efficiency [6], [7]. In these systems, however, the grid voltage is more oscillated than that in the conventional one. Thus, a ride-through control strategy is required for the wind power generation system under the grid fault conditions. For some national grid codes, the wind power systems should keep connected to the grid [3]. In the power system where the wind power generation accounts for a major portion, the grid will experience the power outage if the wind farms trip off. A diagram of the LVRT requirements where wind turbines should stay connected for voltage sags is shown in Fig. 1[3].

Several solutions have been suggested for the LVRT in the DFIG wind turbine systems. For this purpose, a crowbar system is connected in the rotor-side of the DFIG or both the rotor-side and DC bus to absorb the active power during the grid fault [8]-[12]. The wind turbine continues its operation to generate the active power, whereas the reactive power or the voltage at the point of common coupling (PCC) controlled by the GSC for compensating the grid voltage. However, in the case of a weak grid, the GSC cannot supply enough reactive power or voltage support due to the limitation of the power capacity and the risk of voltage instability. Also, the ESS added to the wind generation systems can not offer fault ride-through capability [13]. Nevertheless, the cost of the ESS is not so low to solve this problem practically. Consequently, a braking chopper (BC) which has the low cost and the simple control has been applied for the LVRT [13]-[14]. However, the power quality at the output of the wind turbine systems is not much improved because the BC can just dissipate the power without capability of returning the power to the grid. Another scheme consists of the ESS and the BC which are connected to the DC-link side of the back-to-back converter in a permanent magnet synchronous generator (PMSG) wind turbine system [15]-[16]. With this method, the fault ride-through can be obtained effectively. The power is absorbed from the system or released to the grid for both normal and fault conditions by using the ESS. Meanwhile, the DC-link voltage is controlled at the GSC in both normal condition and grid sags and the power mismatched between the turbine and the grid-side are stored in the inertia by increasing the generator speed. However, the amount of energy stored in the turbine inertia is not so large, when the generator operates near the rated speed before the grid sags happen.

In this paper, a coordinated control strategy for DC-link voltage and crowbar is proposed to enhance the LVRT during the grid fault. The ESS is used to control the DC-link voltage of the back-to-back converters during the grid voltage sags, while the GSC is applied to inject the reactive current according to the grid code requirements. The DC-link capacitor crowbar is used to dissipate the surplus energy. Thus, the grid voltage can be recovered rapidly without an external STATCOM after fault clearance.The validity of the proposed control algorithm is verified by simulation results.

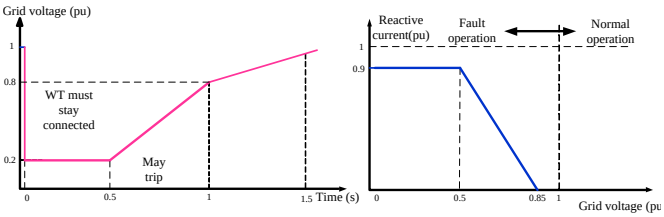


Fig. 1. *Spanish grid code [3]. (a) Low-voltage ride-through requirement. (b) Reactive current requirement.*

*Research was supported by Ho Chi Minh city University of Food Industry.

T. L. Van, H. Tran and N. K. Dang are with the Department of Electrical and Electronic Technology, Ho Chi Minh city University of Food Industry, Ho Chi Minh 700000, Vietnam (Tel: +84-909653157, e-mail: luonghepc@gmail.com, hoantran205@gmail.com, dangngockhoa@gmail.com).

T. H. Truong is with HUTECH Institute of Engineering, HUTECH University of Technology, Ho Chi Minh 700000, Vietnam (e-mail: hieuhepc@gmail.com).

II. COORDINATED CONTROL STRATEGY FOR LVRT

A. Control of GSC

The control block diagram of the GSC is shown in Fig. 2. The operation of the GSC is directly affected by grid voltage sags. In this duration, the wind turbine and generator keep operating as if it is in normal condition. Conventionally, the DC-link voltage is controlled by the GSC. Thus, in the DC-link, power delivered from the generator side may increase the DC-link voltage excessively high. Differently from the conventional control of the AC/DC converter, the DC-link voltage is controlled by the ESS when the grid voltage sags happen. Thus, the GSC is used to control the grid reactive current according to the requirement of the grid code [17]-[18]. Therefore, the reference of the active current component, I_{qe}^{+*}, is set to zero, while the reactive current references (Fig. 1) depending on the levels of the grid voltage drop are expressed as

$$\begin{cases} I_{de}^{+*} = 0.9\,pu & if \;\; 0 \le E_{qe}^{+} \le 0.5\;(pu) \\ I_{de}^{+*} = 2.186 - 2.571E_{qe}^{+} & if \;\; 0.5 \le E_{qe}^{+} \le 0.85\;(pu) \\ I_{de}^{+*} = 0 & if \;\; E_{qe}^{+} \ge 0.85\,(pu) \end{cases} \quad (1)$$

where I_{de}^{+*} is the d-axis current reference of positive-sequence component in *p.u.* and E_{qe}^{+} is the q-axis grid voltage of positive-sequence component.

The *dq*-axis current references of the negative-sequence component, I_{dqe}^{-*}, are set to zero to eliminate the unbalanced current component flowing into the grid, which are expressed as

$$\begin{aligned} I_{qe}^{-*} &= 0 \\ I_{de}^{-*} &= 0 \end{aligned}. \quad (2)$$

B. Control of RSC

Under unbalanced grid voltage sags, the dual rotor current controllers for positive-sequence dq-axis and negative- sequence dq-axis components are applied for the RSC, in which the dq-axis rotor current references of the positive-sequence component are determined by the stator active and reactive power controllers, respectively. Thus, the stator active power reference is obtained from the MPPT method, while the reference of the stator reactive power is set to zero. To eliminate the oscillations in the stator reactive power, its oscillating terms (see in [16]) must be nullified ($Q_{ss}^{*} = Q_{sc}^{*} = 0$).

C. Control of ESS for Constant DC-Link Voltage

At grid sags, the DC-link voltage of the back-to-back converter is controlled by the ESS instead of the GSC. Neglecting the power losses of the converters and considering the active power negligible flowing into the grid, the dynamic equation of the DC-link voltage is expressed as

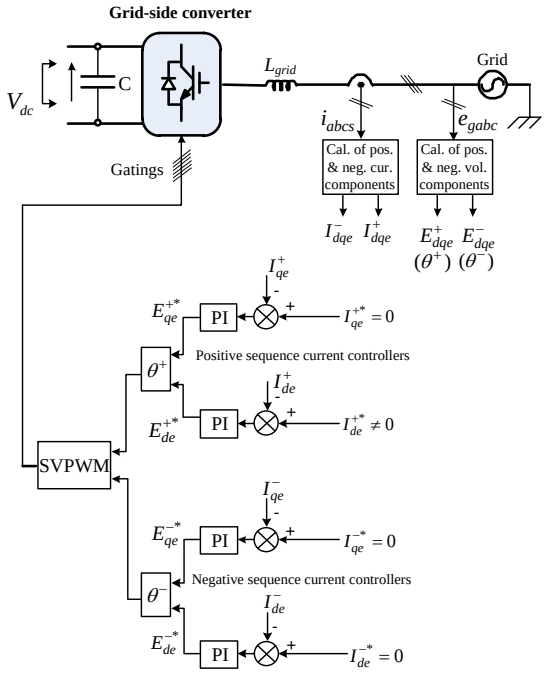


Fig. 2. *Control block diagram of GSC.*

$$P_r - P_{BC} - P_{ESS} = \frac{1}{2} C \frac{dV_{dc}^2}{dt^2} \quad (3)$$

where C is the DC-link capacitance, P_r is the rotor power, P_{BC} is the power dissipated by the crowbar, P_{ESS} is the power of the ESS computed from the ESS voltage, V_{ESS}, and the supercapacitor current, I_{ESS}, as

$$P_{ESS} = V_{ESS} \cdot I_{ESS} \quad (4)$$

From (3), in order to keep the DC-link voltage as constant, the ESS should be able to absorb the generator power fully. For this, selecting the rating of the ESS has been described in detail in [19], in which the rating of the ESS is chosen 30% of the system power rating for reducing the total system cost.

From (3) and (4), we have

$$\frac{dV_{dc}^2}{dt^2} = \frac{2}{C}\left(P_r - P_{BC}\right) - \frac{2V_{ESS}}{C} I_{ESS} \quad (5)$$

A single-input and single-output nonlinear system is expressed as [20], [21]

$$\dot{x} = f(x) + g(x)u \quad (6)$$

$$y = h(x) \quad (7)$$

where x is the state vector, u is the control input, y is the output, f and g are the smooth vector fields, respectively, and h is the smooth scalar function.

The nonlinear equation in Eq. (5) is expressed in the form of Eq. (6) as follows:

$$\ddot{V}_{dc} = \frac{2}{C}\left(P_r - P_{BC}\right) - \frac{2V_{ESS}}{C} I_{ESS} \qquad (8)$$

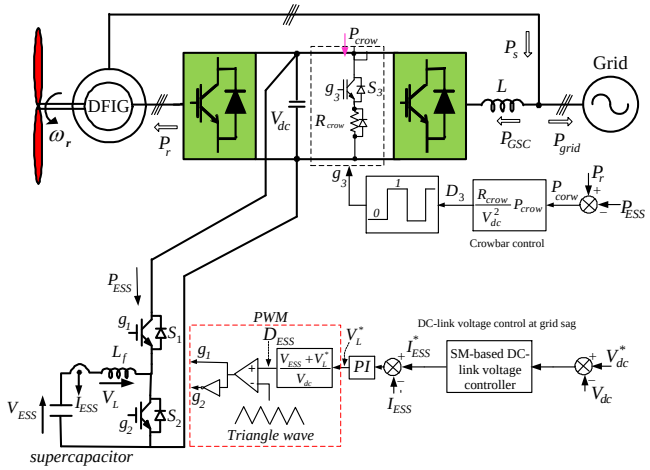


Fig. 3. *Control block diagram of ESS and crowbar.*

By differentiating the output y of the system until input control signal appears, the result is given as

$$\ddot{y} = A(x) + E(x)u \qquad (9)$$

where

$$A(x) = \frac{2}{C}\left(P_r - P_{BC}\right) \text{ and } E(x) = -\frac{2V_{ESS}}{C}$$

If a control input u is chosen as

$$u = E^{-1}(x)\left[-A(x) + v\right] \qquad (10)$$

where v is the equivalent control input to be specified.

The sliding surface (s) is defined as

$$s = \dot{e} + k_1 e + k_2 \int e\,dt \qquad (11)$$

where $e = y - y^*$, y^* is the tracking reference, and k_1, and k_2 are the positive constant gains.

By using a sliding mode control (SM) theory, the equivalent control input can be derived as

$$u = E^{-1}(x)\left[-A(x) - \ddot{e} + k_1\dot{e} + k_2 e\right] + \gamma sign(s) \qquad (12)$$

where γ>0.

The stability and robustness can be tested using Lyapunov's function which is presented in [21].

D. Crowbar Control for Power

During the grid voltage sags, the ESS may not absorb the full generator power, and then the crowbar will be activated to dissipate the rest of the power, P_{crow} as

$$P_{crow} = P_r - P_{ESS} \qquad (13)$$

As shown in Fig. 3, the crowbar is controlled by the switch S_3. The duty ratio D_3 for the switch depends on P_{crow}, which is expressed as

$$D_3 = \frac{R_{crow}}{V_{dc}^2} P_{crow} \qquad (14)$$

where R_{crow} is the crowbar resistance.

III. SIMULATION RESULTS

In order to test the LVRT capability of the wind turbine system, PSCAD simulations have been carried out for a 2-MW DFIG wind turbine system to verify the feasibility of the proposed method. The parameters of the wind turbine and generator are listed in Table 1 and 2, respectively. The switching frequency for the converters is 2[kHz], and the grid voltage is 690[V_{rms}]/60[Hz].

TABLE 1. PARAMETERS OF WIND TURBINE

Rated power	2 [MW]
Blade radius	44.18 [m]
Air density	1.225[kg/m^3]
Max. power conv. coefficient	0.4
Cut-in speed	3[m/s]
Cut-out speed	25[m/s]
Rated wind speed	11 [m/s]
Blade inertia	6.3x10^6[kg.m^2]

TABLE 2. PARAMETERS OF DFIG

Rated power	2 [MW]
Stator voltage/frequency	690 [V]/60 [Hz]
Stator/rotor resistance	0.00488pu/0.00549pu
Stator/rotor leakage inductance	0.0924pu/0.0995pu
Generator inertia	200[kg.m^2]

Fig. 4 shows the performance of the GSC at voltage sags. Fig. 4(a) shows the grid voltage, where three grid-phase voltages drop to 24%, 36%, and 64%, respectively during 0.25[s]. The q-axis grid current of the positive-sequence component is shown in Fig. 4(b), in which it becomes zero during the grid sag since no active power flows into the grid. The reactive current component is injected to the grid as shown in Fig. 4(c). The negative-sequence components of q- and d-axis grid currents are shown in Fig. 4(d) and (e), respectively, in which they are controlled to zero to obtain the balanced grid current as shown in Fig. 4(f).

Fig. 5 shows the response of DFIG wind turbine system under unbalanced grid voltage. The stator and rotor power of the DFIG are shown in Fig. 5(a) and (b), respectively. Due to the reduction of generator power reference, the power difference between the turbine and DFIG power accelerates the system. During the grid faults, the rotor speed is increased, as shown in Fig. 5(d). As illustrated in Fig. 5(e), the generator torque is also reduced and fluctuated due to the unbalanced grid sags.

Fig. 6 shows the performance of the ESS and the crowbar. The DC-link voltage is controlled well as shown in Fig. 6(a), in which its transient value is less than 3.2%. Fig. 6(b) shows the ESS powers, in which the control

performance is good for normal condition. When the grid fault occurs, the power controller is deactivated and the power is absorbed by the ESS as seen in Fig. 6(b) to keep the DC-link voltage. The current control performance is shown in Fig. 6(c). Since the ESS is not able to absorb the full generator power, the rest of the power is dissipated by the crowbar, in which the crowbar current is shown in Fig. 6(d). The super-capacitor voltage is increased as shown in Fig. 6(e).

Fig. 7 shows the comparison of the DC-link voltage control between the conventional method [19] and the proposed one. It can be seen in Fig. 7(a) that, at this fault, the DC-link voltage can not be controlled well by the grid-side converter. The DC-link voltage is increased by about 10%, while the increase of the DC-link voltage (Fig. 7(b)) in the proposed method is less than 3.2 %.

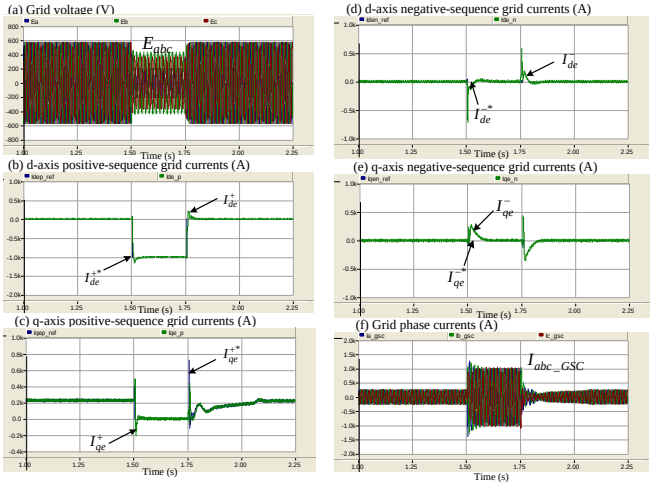


Fig. 4. Performance GSC under unbalanced sag. (a) Grid voltage. (b) q-axis positive-sequence grid currents. (c) d-axis positive-sequence grid currents. (d) q-axis negative-sequence grid currents. (e) d-axis negative-sequence grid currents. (f) Grid phase currents.

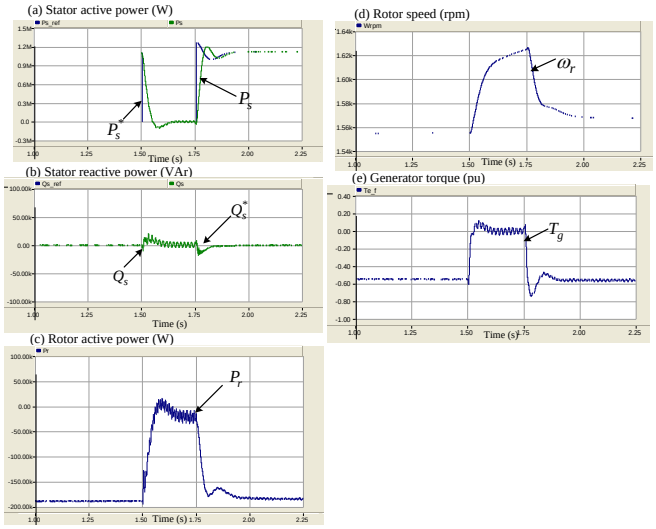


Fig. 5. *Generator performance under unbalanced sag. (a) Stator active power. (b) Stator active power. (c) Rotor active power. (d) Generator speed. (e). Generator torque.*

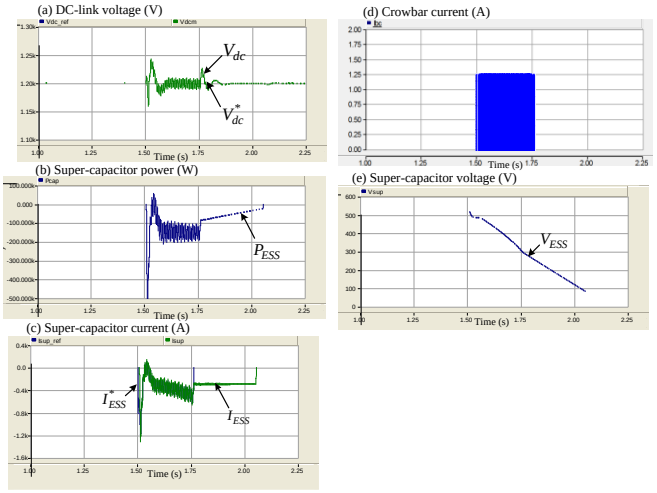


Fig. 6. *Performance of the ESS and crowbar under unbalanced sag. (a) DC-link voltage. (b) Super-capacitor power. (c) Super-capacitor current. (d) Crowbar current. (e) Super-capacitor voltage.*

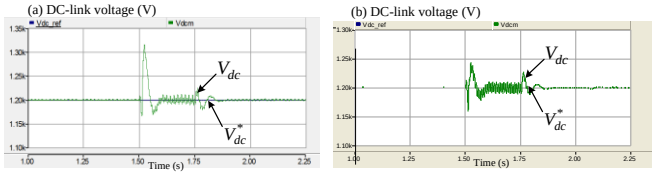


Fig. 7. *Performance of DC-link voltage control in conventional method (a) [18] and proposed method (b).*

IV. CONCLUSION

This paper has proposed a coordinated control strategy for DC-link voltage and crowbar for the LVRT in DFIG wind turbine systems. The DC-link voltage is controlled by the ESS, while the GSC is able to comply with the reactive current requirements of the grid code. By this, the grid voltage can be recovered rapidly without an external STATCOM after fault clearance. The validity of the proposed control algorithm is verified by simulation results for 2 MW DFIG wind power system.

ACKNOWLEDGMENT

This research was supported by Ho Chi Minh City University of Food Industry research grants.

REFERENCES

[1] J. Lopez, E. Gubia, P.Sanchis, X. Roboam, and L. Marroyo, "Wind turbines based on doubly fed induction generator under asymmetrical voltage dips," *IEEE Trans. Energy Convers.*, vol. 23, no. 1, pp. 321-330, 2008.

[2] M. Tsili and S. Papathanassiou, "A review of grid code technical requirements for wind farms," *IET Renew. Power. Gener.*, Vol. 3, No. 3, pp. 308-332, 2009.

[3] F.Iov, A.D. Hansen, P. Sørensen, and N. A. Cutululis, "Mapping of grid faults and grid codes," Technical Report Risø-R-1617(EN), Risø National Laboratory, Technical University of Denmark, Roskilde, Denmark, 2007.

[4] C. Saniter and J. Janning, "Test bench for grid code simulations for Multi-MW wind turbines, design and control," *IEEE Trans. Power Electron.*, vol. 23, no. 4, pp. 1707-1715, 2008.

[5] K. Loudiyia , A. Berradaa, H. G. Svendsenc , K. Mentesidid, "Grid code status for wind farms interconnection in Northern Africa and

Spain: Descriptions and recommendations for Northern Africa," *Renewable and Sustainable Energy Reviews*, vol. 81, pp. 2584-2598, Jan., 2017.

[6] J.-H. Jeon, S.-K. Kim, C.-H.Cho, J.-B. Ahn, and E.-S.Kim, "Development of simulator system for micro-grids with renewable energy sources," *Journal of Electrical Engineering & Technology*, vol. 1, no. 4, pp.409-413, 2006.

[7] Pollin R., Peltier H. G., and H. Scharber, Green recovery: A new program to create good jobs and start building a low-carbon economy, Center for American Progress, 2008.

[8] F. K. A. Lima, A. Luna, P.Rodriguez, E. H. Watanabe, and F. Blaabjerg, "Rotor voltage dynamics in the doubly fed induction generator during grid faults," *IEEE Trans. Power Electron.*, vol. 25, no. 1, pp. 118-130, 2010.

[9] L. G. Meegahapola, T. Littler, and D.Flynn, "Decoupled-DFIG fault ride-through strategy for enhanced stability performance during grid faults," *IEEE Trans. Sustainable Energy*, vol. 1, no. 3, pp. 2178-2192, 2010.

[10] G. N. Sava, S. Costinas, N. Golovanov, S. Leva, D. M. Quan, "Comparison of active crowbar protection schemes for DFIGs wind turbine," in *Proc. IEEE 16th International Conference on Harmonics and Quality of Power*, 2014, pp. 669–673.

[11] A. Wang, W. Xi, and Y. Alsmadi, "Performance Comparison of LVRT Techniques for DFIG Wind Turbine Under Asymmetrical Voltage Sags," *IEEE 11th International Conference on Power Electronics and Drive Systems (*PEDS 2015*)*, 2015, pp. 254-258.

[12] A. M. A. Haidar, K. M. Muttaqi, and M. T. Hagh, "A Coordinated Control Approach for DC link and Rotor Crowbars to Improve Fault Ride-Through of DFIG based Wind Turbines," *IEEE Trans. Ind. App.*, vol. 53, no. 4, pp. 4073-4086, Jul-Aug., 2017.

[13] C. Abbey and G. Joos, "Supercapacitor energy storage for wind energy applicatons," *IEEE Trans. Ind. App.*, vol. 43, no. 3, pp. 769-776, 2007.

[14] J. F. Conroy and R. Watson, "Low-voltage ride-through of a full converter wind turbine with permanent magnet generator," *IET Renew. Power. Gener.*, Vol. 1, No. 3, pp. 182-189, 2007.

[15] W. Li, C. Abbey, and G. Joos, "Control and performance of wind turbine generators based on permanent magnet synchronous machines feeding a diode rectifier," *Proc. of IEEE PESC*, 2006, pp.1-6.

[16] S. Alepuz, A. Calle, S. B. Monge, J. Bordonau, S. Kouro, and B. Wu, "Control scheme for low voltage ride-through compliance in back-to-back NPC converter based wind power systems," *IEEE International Symposium on Industrial Electronics(ISIE'10)*, 2010, pp. 2357-2362.

[17] K. Li, J. Liu, Z. Wang, and B. Wei, Strategies and operating point optimization of STATCOM control for voltage unbalanced mitigation in three-phase three-wire systems, IEEE Trans. Power Del., vol. 22, no. 1, pp. 413-422, 2007.

[18] M. N. Slepchenkov, K. M. Smedley, and J. Wen, "Hexagram-converter-based STATCOM for voltage support in fixed-speed wind turbine generation systems," *IEEE Trans. Ind. Electron.*, vol. 58, no. 4, pp. 1120-1131, 2011.

[19] T. H. Nguyen and D. C. Lee, "Improved LVRT capacity and power smoothening of DFIG wind turbine systems," *Journal of Power Electronics*, vol. 11, no. 4, pp. 568-575, 2011.

[20] T. L. Van, N. M. D. Nguyen, L. T. Toi and T. T. Trang, "Advanced Control Strategy of Dynamic Voltage Restorers for Distribution System Using Sliding Mode Control Input-Ouput Feedback Linearization", *Lecture notes in electrical engineering*, Vol. 465, pp.521-531, Dec., 2017.

[21] J. J. E. Slotine and W. Li, *Applied Nonlinear Control*. Englewood Cliffs, NJ: Prentice-Hall, 1991, pp. 207–271.